

EXTRACTION AND SPRAY-DRYING CHLOROPHYLL FROM *Chaetomorpha aerea* ALGAE

Hoang Thi Ngoc Nhon*, Nguyen Hoang Bao Ngan, Ho Phung Thanh Doanh

Ho Chi Minh City University of Industry and Trade

*Email: nhonhtn@huit.edu.vn

Received: 26 May 2025; Accepted: 25 June 2025

ABSTRACT

Chaetomorpha aerea is a filamentous green alga commonly found in saline and brackish aquaculture environments, where its excessive proliferation poses ecological concerns and operational challenges. Utilizing this abundant biomass for chlorophyll extraction offers a sustainable biorefinery approach, mitigating environmental impacts while enabling the recovery of high-value bioactive compounds, as the species contains notably high chlorophyll content. Chlorophyll, a natural pigment essential for photosynthesis, is widely applied as a functional additive in food and cosmetic products due to its antioxidant, antibacterial, antifungal, hepatoprotective, anticancer, and immunomodulatory properties. This study investigated the effects of MgCO_3 concentration, microwave power, and extraction time on chlorophyll extraction from *C. aerea* using microwave-assisted extraction (MAE). A Box-Behnken design was applied to optimize the conditions, which were determined to be 0.8% MgCO_3 , 360 W, and 240 s, yielding 50.831 $\mu\text{g/mL}$ of chlorophyll - closely aligned with model predictions. The extract was concentrated under vacuum at 48 °C to 12% total solids, mixed with maltodextrin (25%), and spray-dried at 160°C with a feed rate of 8 mL/min. The final powder exhibited a green color, 3.37% moisture, good water solubility, and a recovery yield of 72.98%. Compared to previous studies, MAE increased chlorophyll yield by approximately 1.5 times, while spray-drying nearly doubled recovery efficiency, highlighting the effectiveness of this integrated extraction and stabilization strategy.

Từ khóa: Box-Behnken, *Chaetomorpha aerea*, chlorophyll, optimization, spray-drying.

1. INTRODUCTION

In response to the increasing demand for natural colorants as alternatives to synthetic dyes, which may pose health and environmental risks, chlorophyll has emerged as a promising candidate due to its safety and biodegradability [1]. Beyond fulfilling the requirement for natural coloration, chlorophyll has attracted considerable attention for its beneficial bioactivities, including antioxidant, anti-inflammatory, and antimicrobial properties [2]. These attributes extend its potential applications across functional foods, cosmetics, and pharmaceutical products. Consequently, the exploitation and development of chlorophyll-based products contribute significantly to advancing sustainable solutions within the modern bioprocessing industry.

Chlorophyll is a widely distributed natural pigment found in photosynthetic organisms ranging from prokaryotic bacteria to higher plants. It predominantly occurs in cyanobacteria, algal chloroplasts, and terrestrial plant tissues, where it plays a central role in photosynthesis by absorbing light energy and converting it into biochemical energy [3]. In addition to its photosynthetic function, chlorophyll and its derivatives have been extensively investigated for diverse biological activities, notably antioxidant, anti-inflammatory, and anticancer effects, demonstrating pronounced efficacy against hepatocellular carcinoma and breast cancer cell lines [4].

Green macroalgae serve not only as a source of essential nutrients and feed for aquatic organisms but also possess a broad spectrum of bioactive compounds with immunomodulatory, antimicrobial, and antioxidant potential [5]. Among these, *Chaetomorpha aerea* (*C. aerea*), a filamentous green alga of the *Cladophoraceae* family, is widely distributed in brackish water ecosystems in Vietnam [6]. While

this species may contribute positively to aquaculture food chains, its overgrowth and decomposition can degrade water quality, posing a threat to aquatic farming systems. Given the growing demand for functional ingredients from sustainable and underutilized biomass, *C. aerea* represents a promising candidate for chlorophyll extraction. However, studies focusing on chlorophyll recovery from this species remain limited.

Microwave-assisted extraction (MAE) has emerged as an efficient and environmentally friendly technique for isolating thermolabile compounds, offering advantages such as shortened extraction time, reduced solvent usage, and improved yields [7, 8]. Since chlorophyll is photosensitive [9] and susceptible to oxidative degradation [10], process optimization and stabilization strategies, —such as encapsulation via spray drying with maltodextrin, —are necessary to preserve its structural integrity and functional properties during downstream processing. Previous studies have successfully applied MAE for chlorophyll extraction from various botanical sources, including *Pandanus amaryllifolius* and *Chlorella vulgaris* [11, 12]. Nevertheless, systematic studies on optimizing chlorophyll extraction and stabilization from *C. aerea* are scarce.

In particular, the addition of MgCO_3 during microwave-assisted extraction has been widely investigated, demonstrating its role in protecting the pigment from thermal and oxidative degradation, thereby enhancing chlorophyll recovery yields [13] and preserving its characteristic green color [14].

Specifically, spray drying has been widely applied to stabilize chlorophyll due to its effectiveness in reducing moisture and protecting sensitive compounds. Among encapsulating agents, maltodextrin is frequently used owing to its low cost, high efficiency, bland taste, low viscosity at high solid content, and excellent water solubility [15]. This approach has been shown to effectively stabilize physicochemical properties and biological activities of hydrophobic and unstable compounds like chlorophyll [16, 17]. Moreover, spray-drying-based microencapsulation helps minimize interactions between powder constituents and environmental factors, thereby enhancing overall product stability [18].

Despite the widespread application of microwave-assisted extraction and spray drying techniques for recovering and stabilizing chlorophyll from *C. aerea*, systematic optimization of the extraction process remains insufficiently explored. Notably, the use of advanced experimental designs - such as Box-Behnken to simultaneously evaluate and optimize extraction parameters has been rarely reported. This study addresses these gaps by employing a Box-Behnken design to investigate the effects of magnesium carbonate (MgCO_3) concentration, microwave power, and extraction time on the efficiency of chlorophyll extraction, aiming to maximize yield while preserving bioactivity. The developed predictive regression model was validated experimentally to confirm the optimal extraction conditions. Furthermore, the influence of spray drying parameters on the physicochemical properties and functional stability of the chlorophyll powder was thoroughly examined to produce a stable, high-quality product. The findings contribute to establishing a robust and scalable extraction protocol for producing chlorophyll-enriched ingredients suitable for functional foods and nutraceutical applications.

2. MATERIALS AND METHODS

2.1. Materials

2.1.1. Materials

C. aerea algae was collected from shrimp ponds in Gia Ray town, Bac Lieu province. The collected algae were transported in foam boxes to the laboratory on the same day. At the laboratory, it was washed to remove impurities, then dried and finely ground by machine crushing the dry algae to a particle size of around 0.5 mm before storing it at 4 °C until usage.

2.1.2. Chemicals

Magnesium carbonate (Xilong Scientific Co., Ltd., China), ethanol (Xilong Scientific Co., Ltd., China), maltodextrin (Cool Chemistry, China).

2.2. Methods

2.2.1. Preparing *C. aerea* powder

The algae were thoroughly washed to remove impurities, followed by drying at 60 °C for 6-7 h until the moisture content dropped below 10%. The dried samples were then ground to pass through an 80-mesh sieve.

2.2.2. Effects of chlorophyll extraction from *C. aerea*

One g of *C. aerea* powder (according to the dry mass) was added with distilled water at a 1:10 (w/v) in the investigated concentrations of MgCO₃ (0.2, 0.4, 0.6, 0.8, 1.0 %w/w), in different microwave powers (90, 180, 270, 360, 450 W) and different microwave times (60, 120, 180, 240, 300 s). Afterwards, microwave-treated samples were added ethanol to reach 60% concentration before being incubated at 60 °C for 60 min and centrifuged at 5000 rpm for 15 min. The supernatant was analyzed spectrophotometrically to determine total chlorophyll content and evaluate the optimal concentration of MgCO₃ and microwave-treated conditions.

2.2.3. Optimal experimental design

Response surface methodology (RSM) was employed to simultaneously optimize multiple variables to achieve the desired response. A Box-Behnken design with 15 experimental runs, including 3 replicates at the centre point, was applied to determine the optimal extraction conditions. The independent variables evaluated were MgCO₃ concentration, microwave power, and microwave irradiation time, all of which influenced the chlorophyll content. The response variable, chlorophyll yield, was assessed, and a second-order polynomial model was used to describe the relationship between the response (Y) and the independent variables (X_i).

$$Y_i = b_0 + b_1X_1 + b_2X_2 + b_3X_3 + b_{12}X_1X_2 + b_{13}X_1X_3 + b_{23}X_2X_3 + b_{11}X_1^2 + b_{22}X_2^2 + b_{33}X_3^2 \quad (\text{Eq.1})$$

The extract obtained under optimized conditions was subsequently used to investigate the parameters of the spray drying process.

2.2.4. Effects of spray drying on obtaining chlorophyll powder

The chlorophyll extract was concentrated through rotary evaporation at 48 °C to completely remove the solvent completely. Subsequently, it was mixed with different maltodextrin at carrier concentrations of 15%, 20%, 25%, and 30% (w/w, based on sample weight), aiming to increase the total solid content to 12%. The mixtures were then subjected to spray drying at inlet temperatures (140, 150, 160, 170 °C) with different feed rates (6, 7, 8, 9 mL/min).

2.3. Analytical methods

2.3.1. Determination of chlorophyll content

Chlorophyll content was determined using the spectrophotometry method, referencing Iain *et al.*, (1995). Chlorophyll exhibits maximum light absorption at 645 nm and 663 nm wavelengths, reflecting the amount of chlorophyll present in the solution.

$$\text{Total chlorophyll } (\mu\text{g/L}) = 20.2 \times A_{645} + 8.02 \times A_{663} \quad (\text{Eq.2})$$

where A_{645} and A_{663} are the absorbance values of chlorophyll at 645 nm and 663 nm, respectively.

2.3.2. Determination of chlorophyll powder recovery

The chlorophyll powder yield after spray drying was calculated based on the dry weight using the following formula [19]:

$$\text{Chlorophyll powder recovery } (\%) = \left(\frac{\text{obtained spray dried (g)}}{\text{chlorophyll extract (g) + maltodextrin (g)}} \right) \times 100 \quad (\text{Eq.3})$$

2.3.3. Determination of chlorophyll powder properties

Bulk density (Bd): Bulk density (g/cm³) of the chlorophyll powder was assessed by placing 2 g of the sample into a 10 mL graduated cylinder and recording the volume it occupied. The density was then calculated by dividing the sample's weight by its volume, as outlined by Saifullah *et al.*, (2016) [20].

Particle density (Pd): To evaluate the density of chlorophyll powder, 1 g of the powder was transferred into a 10 mL graduated cylinder sealed with a glass stopper. Then, 5 mL of petroleum ether

was added, and the cylinder was shaken for around 30 s to suspend all particles. An additional 2 mL of petroleum ether was used to rinse the inner walls of the cylinder. The total volume of the petroleum ether and suspended particles was recorded, and the powder density was calculated as the ratio of the powder's mass to this measured volume [21].

Tapped density (Td): Tapped density was determined by placing 2.5 g of chlorophyll powder into a 10 mL graduated cylinder. The cylinder was then tapped manually 100 times from a height of 15 cm onto a rubber surface to allow powder compaction. The final volume was recorded, and tapped density (g/cm³) was calculated by dividing the powder weight by the compacted volume [20].

Solubility (S): One gram of the chlorophyll powder was dispersed in 100 mL of distilled water and stirred using a magnetic stirrer at 500 rpm for 30 min. The resulting mixture was transferred into centrifuge tubes and centrifuged at 2214 g for 5 min (Model Z 206A, HermLe, Germany). The collected supernatant was dried at 105 °C for 5 h in a hot air oven, and solubility (%) was determined by comparing the dried residue weight to the original powder mass [21].

Flowability (F): The flowability of the samples was assessed using the Carr Index (CI) and Hausner Ratio (HR), which were calculated based on the measured bulk density (Bd) and tapped density values [20].

$$CI (\%) = \frac{Td - Bd}{Td} \times 100 \text{ (Eq.4)}$$

$$HR = \frac{Td}{Bd} \times 100 \text{ (Eq.5)}$$

Porosity (P): The porosity (P) of the chlorophyll powder was calculated using particle density (Pd) and tapped density (Td) [21].

$$P (\%) = \frac{Pd - Td}{Pd} \times 100 \text{ (Eq.6)}$$

2.3.4. Structural and morphological analysis

Fourier transforms infrared spectroscopy (FT-IR)

The infrared spectrum of chlorophyll powder was obtained using a Tensor 37 FT-IR spectrometer (Bruker, Germany). Spectral data were collected within the wavenumber range of 4000 to 450 cm⁻¹, at a resolution of 1 cm⁻¹, with a total of 100 scans recorded at a scan rate of 0.5 cm⁻¹/s. For analysis, the sample was finely ground, mixed with potassium bromide (KBr), and compressed into a pellet. A pure KBr pellet served as the background reference.

Scanning electron microscopy (SEM)

The surface morphology of the chlorophyll powder was examined using a scanning electron microscope (SEM, JEOL). Each sample was individually mounted onto gold-coated aluminium stubs using double-sided adhesive tape. The mounted specimens were then placed in the SEM chamber and observed under an accelerating voltage of 2.5 kV to evaluate particle shape and surface characteristics.

X-ray diffraction (XRD)

The crystalline properties of the chlorophyll powder were analyzed using X-ray diffraction (XRD) with a D2 Phaser diffractometer (Bruker, Germany). Diffraction patterns were recorded within a 2 θ range of 30° to 40°. The analysis was conducted using CuKα radiation with a nickel filter, operated at 40 kV and 0.8 mA. The scan rate was set at 4° per minute to assess the degree of crystallinity.

2.3.5. Microbiological tests

The aerobic colony counts in chlorophyll powder samples were determined by ISO 4833-1:2013. and ISO 21526-2:2008 of yeast and mold in select foods.

2.3.6. Heavy metals test

Heavy metals in chlorophyll powder samples were analyzed according to AOAC Official Method 2015.01, including arsenic (As), lead (Pb), mercury (Hg), and cadmium (Cd).

2.4. Data analysis

All experiments were conducted in triplicate. The results were analyzed and visualized using Microsoft Excel 2019 (USA). Statistical analysis was performed using JMP pro 17 software (USA), and differences between samples were evaluated by one-way analysis of variance (ANOVA) at a significance level of $p < 0.05$.

3. RESULTS AND DISCUSSION

3.1. Microwave-assisted extraction of chlorophyll

The effects of the concentration of MgCO_3 , microwave power and microwave time on chlorophyll extraction are shown in Fig. 1. The chlorophyll content increased progressively from 20.32 $\mu\text{g/mL}$ to 33.02 $\mu\text{g/mL}$ between 0-0.8%, followed by a slight decrease at 1%, reaching $32.43 \pm 0.03 \mu\text{g/mL}$ (Fig. 1A). The results indicated that the chlorophyll content increased progressively with MgCO_3 concentration and reached its peak at 0.8% (w/w), corresponding to $33.02 \pm 1.35 \mu\text{g/mL}$. Although no significant difference was observed among the MgCO_3 concentrations of 0.6%, 0.8%, and 1.0% ($p > 0.05$), the 0.8% level was selected due to its higher average chlorophyll content compared to 0.6%, as well as its ability to provide better protective efficacy. At the 0.6% concentration, the amount of Mg^{2+} ions may be insufficient to prevent the loss of the central Mg^{2+} ion in the chlorophyll molecule, thereby reducing extraction efficiency. The addition of MgCO_3 positively influences chlorophyll extraction by maintaining an excess of Mg^{2+} ions in the extraction medium, which helps to stabilize the chlorophyll structure by preventing demetallation. Conversely, increasing the concentration to 1.0% did not enhance extraction efficiency and tended to decrease chlorophyll yield, likely due to the formation of pheophytins under mildly acidic conditions. This decline is attributed to the acid-catalyzed conversion of chlorophyll into pheophytins, which compromises pigment integrity [22].

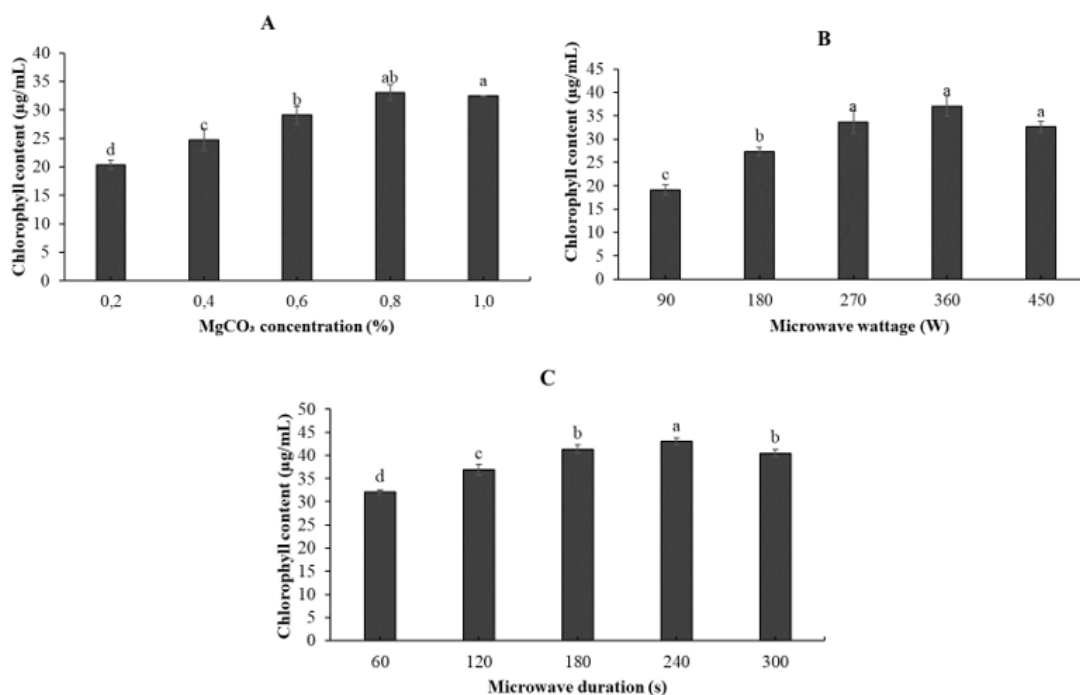


Figure 1. Effect of the concentration of MgCO_3 (A), microwave power (B) and microwave time (C) on chlorophyll extraction ($p < 0.05$; $n=3$)

The results, presented in Fig. 1B, indicate that the efficiency of chlorophyll extraction assisted by microwave treatment was influenced by the applied microwave wattages. As the microwave power increased from 90 to 360 W, the chlorophyll content rose continuously from 19.12 $\mu\text{g/mL}$ to 33.70 $\mu\text{g/mL}$, reaching a peak of $37.09 \pm 2.22 \mu\text{g/mL}$ at 360 W. The rapid heating effect, causing the speedy solvent evaporation and sudden pressure gain, promotes the breakdown of cell structures, facilitating

the release of intracellular compounds into the solvent [23]. Although a statistically no significant difference was observed between chlorophyll extraction at 360 W and 450 W ($p > 0.05$), the power of 360 W was selected due to its energy efficiency and because it yielded the highest chlorophyll content compared to 450 W. Nonetheless, increasing the power to 450 W resulted in a decrease in chlorophyll content, likely due to thermal degradation or transformation of chlorophyll compounds caused by excessive energy input. Supporting findings by Nguyen Hong Khoi Nguyen *et al.*, (2021) also demonstrated a maximum chlorophyll yield of $13.67 \mu\text{g/mL}$ at 360 W [24], suggesting that the result of 360 W is acceptable and suitable for subsequent experiments. Microwave treatment time significantly influenced the amount of chlorophyll extracted. Experimental data show that at 360 W for 240 s, chlorophyll yield reached a maximum of $43.04 \pm 0.76 \mu\text{g/mL}$, but decreased to $40.5 \pm 0.75 \mu\text{g/mL}$ at 300 s. A short exposure time may be insufficient for solute migration from inside the cells to the solvent, whereas an appropriate duration allows solutes to reach equilibrium more efficiently. This trend is clearly illustrated in Fig. 1C, where the chlorophyll content initially increases with time but declines beyond the optimal point, indicating possible thermal degradation or structural damage to the plant matrix. Regardless, extending treatment time does not enhance extraction and even leads to degradation due to high temperature and pressure [25]. Compared to the study carried out by Nguyen Hong Khoi Nguyen *et al.*, (2021), chlorophyll extraction from *Pandanus amaryllifolius* Roxb. under the same duration yielded 3.3 times lower, at $13.03 \mu\text{g/mL}$ [24], demonstrating the superior extraction potential of this algae species.

Overall, the experimental findings indicated that a MgCO_3 concentration of 0.8% (w/w), microwave power of 360 W, and an extraction time of 240 s produced the highest chlorophyll yield under the investigated conditions. These values represent the most favourable parameters within the tested range and will be employed as the foundation for subsequent optimization experiments. The data obtained provide essential insights for refining the extraction process, with the goal of improving efficiency and maximizing chlorophyll recovery in future studies.

3.2. Optimization of chlorophyll extraction process by microwave-assisted extraction using RSM

A response surface methodology (RSM) based on the Box-Behnken design (BBD) was employed to investigate the influence of key parameters on microwave-assisted chlorophyll extraction. Three independent variables were selected: magnesium carbonate concentration (X_1 , %), microwave power (X_2 , W), and extraction time (X_3 , s) (Table 1). Each factor was studied at three levels centred around the midpoints of their respective ranges to construct a predictive quadratic model for chlorophyll content.

Table 1. The variables and levels of BBD for MAE of total chlorophyll from *C. aerea*

Factor Levels	X_1 , Concentration of MgCO_3 (%)	X_2 , Microwave power (W)	X_3 , Microwave time (s)
-1	0.6	270	180
0	0.8	360	240
1	1	450	300

The experimental chlorophyll concentrations obtained from the 15 designed runs (each conducted in triplicate) revealed significant variation across conditions. The highest chlorophyll yield was recorded in run 14 ($50.970 \pm 0.23 \mu\text{g/mL}$), whereas the lowest was observed in run 7 ($40.951 \pm 0.73 \mu\text{g/mL}$). Notably, three central runs (experiments 13 to 15), corresponding to X_1 : 0.8%, X_2 : 360 W, and X_3 : 240 s, consistently produced chlorophyll contents near the predicted optimum, with statistical significance ($p < 0.05$) compared to other treatments.

Analysis of variance (ANOVA) confirmed the adequacy of the quadratic regression model generated by JMP Pro 17 software. The model exhibited a high coefficient of determination ($R^2 = 0.987$), indicating that over 99% of the variation in chlorophyll yield could be explained by the model. The lack-of-fit test ($p = 0.341 > 0.05$) suggested that the deviation of the model from experimental data was not statistically significant, further validating its reliability for prediction.

Table 2. BBK with three independent variables for MAE of total chlorophyll from *C. aerea* residue

Run	Factor 1		Factor 2		Factor 3		Total chlorophyll (µg/mL)	
	X ₁ (%)	Coded X ₁	X ₂ (W)	Coded X ₂	X ₃ (s)	Coded X ₃	Actual value	Predicted value
1	0.6	-1	270	-1	240	0	43.913 ± 0.46	43.986
2	1	1	270	-1	240	0	44.941 ± 0.16	45.273
3	0.6	-1	450	1	240	0	44.929 ± 0.11	44.597
4	1	1	450	1	240	0	40.982 ± 0.56	40.909
5	0.6	-1	360	0	180	-1	44.980 ± 0.10	44.679
6	1	1	360	0	180	-1	43.015 ± 0.23	42.455
7	0.6	-1	360	0	300	1	40.951 ± 0.73	41.511
8	1	1	360	0	300	1	41.033 ± 0.34	41.334
9	0.8	0	270	-1	180	-1	45.974 ± 0.33	46.202
10	0.8	0	450	1	180	-1	45.753 ± 0.69	46.387
11	0.8	0	270	-1	300	1	46.754 ± 0.08	46.120
12	0.8	0	450	1	300	1	42.409 ± 0.15	42.181
13	0.8	0	360	0	240	0	50.506 ± 0.17	50.769
14	0.8	0	360	0	240	0	50.970 ± 0.23	50.769
15	0.8	0	360	0	240	0	50.831 ± 0.23	50.769

The fitted second-order polynomial model describing the relationship between the response and independent variables is presented below:

$$\text{Chlorophyll content (}\mu\text{g/mL)} = 50.769 + 0.525X_1 + 1.311X_2 - 0.447X_3 - 2.153X_1^2 - 1.175X_2^2 - 3.622X_3^2 - 0.494X_1X_2 + 0.012X_1X_3 - 0.281X_2X_3$$

Table 3. ANOVA for response surface quadratic model

Source	Sum of Squares	df	Mean Square	F-value	p-value	
Model	82.4927	9	9.1659	97.96	≤0.001	significant
X ₁ – Concentration of MgCO ₃	2.2029	1	2.2029	23.54	0.005	
X ₂ - Microwave power	13.7576	1	13.7576	147.04	0.000	
X ₃ - Microwave time	1.5976	1	1.5976	17.07	0.009	
X ₁ X ₂	17.1114	1	17.1114	182.88	0.000	
X ₁ X ₃	5.0977	1	5.0977	54.48	0.001	
X ₂ X ₃	48.4256	1	48.4256	517.57	0.000	
X ₁ ²	0.9752	1	0.9752	10.42	0.023	
X ₂ ²	0.0006	1	0.0006	0.01	0.942	
X ₃ ²	0.3158	1	0.3158	3.38	0.126	
Residual	0.4678	5	0.0936			
Lack of Fit	0.3544	3	0.1181	2.08	0.341	not significant
Pure Error	0.1134	2	0.0567			
Cor Total	82.9605	14	0.0936			

Among all the variables, X₂ (microwave power) exerted the strongest individual influence on chlorophyll yield (F = 147.04, p < 0.001), followed by X₁ (MgCO₃ concentration) and X₃ (extraction time). Interaction terms, particularly X₂X₃ and X₁X₂, showed the highest F-values, indicating synergistic

or antagonistic effects depending on the conditions. In contrast, the square term X_2^2 was not statistically significant ($p > 0.9$), suggesting a linear effect of microwave power in the studied range.

This model demonstrated strong statistical significance ($F = 97.96$; $p < 0.001$), implying a meaningful relationship between the predictors and chlorophyll content. The three-dimensional response surface plots (Fig. 2) illustrated interactions between pairs of factors while holding the third constant at its centre point. These plots provided a visual insight into how individual and interactive effects influenced extraction efficiency. For example, combinations of higher microwave power and optimal MgCO_3 concentration enhanced chlorophyll yield, while prolonged exposure time beyond a certain threshold led to degradation.

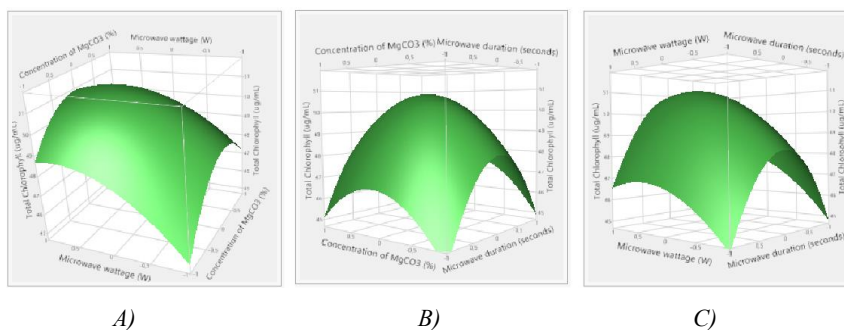


Figure. 2. Response surface plots showing the interactive effects of extraction parameters on total chlorophyll yield ($\mu\text{g/mL}$). (A) Effects of MgCO_3 concentration (%) and microwave power (W) at constant extraction time (240 s); (B) Effects of MgCO_3 concentration (%) and microwave time (s) at constant microwave power (360 W); (C) Effect of microwave power (W) and microwave time (s) at constant MgCO_3 concentration (0.8%).

The response surface plots presented in Fig. 2 illustrate the interactive effects of each pair of independent variables on the total chlorophyll content under microwave-assisted extraction conditions based on the Box-Behnken design model. Fig. 2A demonstrates the interaction between MgCO_3 concentration (%) and microwave power (W) while microwave time is held constant at 240 s. The response surface indicates an increase in chlorophyll content as the MgCO_3 concentration increases from 0.6% to 0.8%, and microwave power increases from 270 W to 360 W. However, a further increase in power to 450 W leads to a slight reduction in chlorophyll content, especially at higher MgCO_3 levels (1.0%). This trend is supported by the experimental data, where a condition of 1.0% MgCO_3 , 450 W, and 240 s yielded $40.98 \pm 0.56 \mu\text{g/mL}$, which is among the highest recorded values, second only to the central point condition (0.8% – 360 W – 240 s) with $50.97 \pm 0.23 \mu\text{g/mL}$. Fig. 2B reveals the effects of MgCO_3 concentration (%) and microwave time (s) when microwave power is fixed at 360 W. Chlorophyll content increases as both factors rise, reaching a maximum of 0.8% MgCO_3 and 240 s, corresponding to experimental values of 50.83 – $50.97 \mu\text{g/mL}$. Beyond these optimal conditions, further increases in MgCO_3 concentration or extraction time slightly reduce the yield, potentially due to thermal degradation or oxidation of chlorophyll. Fig. 2C illustrates the interaction between microwave power (W) and microwave time (s) at a fixed MgCO_3 concentration of 0.8%. Chlorophyll content increases as power increases from 270 W to 360 W and time from 180 s to 240 s. However, at 450 W, the response declines notably. For instance, the condition of 0.8% – 450 W – 300 s resulted in only $42.41 \pm 0.15 \mu\text{g/mL}$, approximately $4.3 \mu\text{g/mL}$ lower than the central point, highlighting the adverse effect of excessive power on chlorophyll stability, possibly due to thermal degradation or pigment breakdown.

Collectively, the response surfaces indicate a pronounced nonlinear behaviour and highlight the significance of interaction effects between variables. The optimal condition was identified at 0.8% MgCO_3 , 360 W, and 240 s, with an actual chlorophyll content of 50.83 – $50.97 \mu\text{g/mL}$, closely matching the predicted value of $50.77 \mu\text{g/mL}$.

The adequacy and robustness of the fitted model were further validated through diagnostic plots. The normal probability plot of standardized residuals (Fig. 3A) closely followed a straight line, indicating that the residuals were normally distributed and supporting the validity of the ANOVA assumptions. Furthermore, the predicted versus actual plot (Fig. 3B) demonstrated strong agreement between experimental and model-predicted chlorophyll concentrations. Most data points fell within the 75%–90% range, closely aligning with the observed values. The high coefficient of determination (R^2

= 0.994) observed in this plot further confirmed the model's strong predictive capability. Collectively, the small p-values associated with the main effects and interaction terms ($p < 0.05$) reinforced the statistical significance of the model and underscored the contribution of these variables to the overall extraction efficiency.

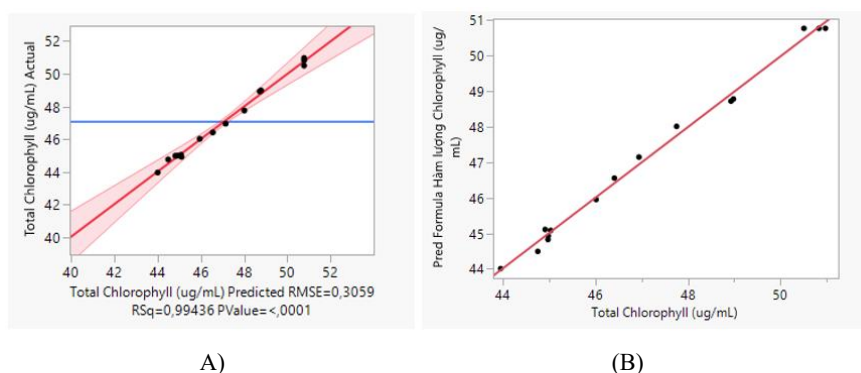


Figure 3. Diagnostic plots for model validation: (A) Normal probability plot of residuals indicating normal distribution and model adequacy; (B) Plot of actual vs. predicted chlorophyll concentrations ($\mu\text{g/mL}$) showing strong agreement between values

The negligible difference ($p > 0.05$) confirms the reliability of the second-order regression model, supporting its applicability in predicting and optimizing chlorophyll extraction using microwave-assisted techniques. Based on the model prediction and desirability analysis, the optimal conditions for maximum chlorophyll recovery were determined to be X_1 : 0.8% MgCO_3 , X_2 : 360 W, and X_3 : 240 s. Under these conditions, the experimental chlorophyll yield reached $50.97 \pm 0.23 \mu\text{g/mL}$, closely matching the predicted value of $50.77 \mu\text{g/mL}$ with no significant difference ($p > 0.05$). This alignment between predicted and actual values confirms the model's validity and practical applicability for optimizing microwave-assisted chlorophyll extraction. Moreover, this optimization process facilitates achieving the highest recovery efficiency during subsequent spray drying and ensures the functional and physical properties of the resulting powder are reliable and suitable for further application studies.

3.3. Spray drying process for chlorophyll powder recovery

The effects of spray-drying to obtain chlorophyll from *C. aerea* extract are shown in Fig. 4.

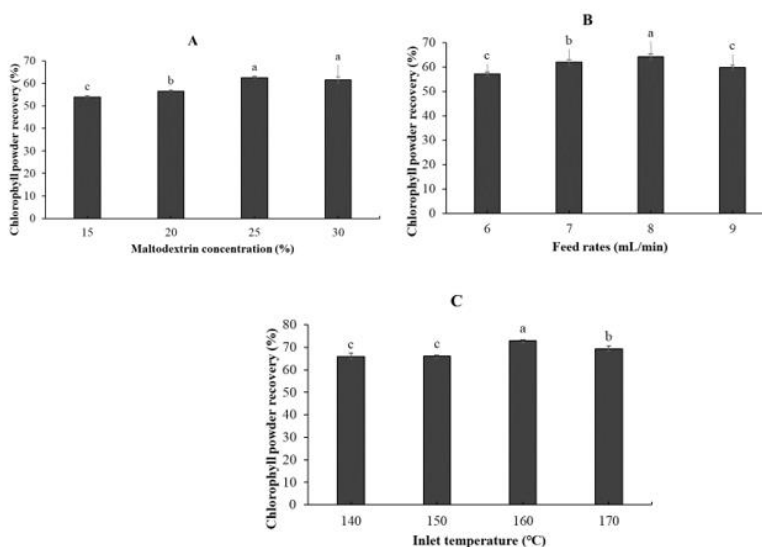


Figure 4. Effect of maltodextrin concentration (%) (A), feed rates (mL/min) (B) and inlet temperature ($^{\circ}\text{C}$) (C) on the recovery yield of chlorophyll.

Fig. 4A illustrates the effect of maltodextrin concentration on the recovery yield and physical characteristics of the spray-dried powder. As the carrier concentration increased from 15% to 25%, the powder recovery yield improved progressively, reaching a peak value of $62.63 \pm 0.54\%$ at 25%. Although no significant difference was observed between carrier concentrations of 25% and 30% ($p > 0.05$), the 25% concentration was selected to reduce chemical usage while achieving the highest chlorophyll recovery yield. Moreover, further increasing the carrier concentration to 30% resulted in a slight decline in yield ($61.60 \pm 1.35\%$), which may be attributed to increased feed viscosity and decreased drying efficiency. At lower maltodextrin levels, significant powder deposition on the inner wall of the drying chamber was observed, reducing product recovery. The increase in maltodextrin concentration significantly influences the recovery yield of chlorophyll powder during spray drying. At an optimal concentration, maltodextrin raises the glass transition temperature (T_g) of the mixture, reducing product stickiness on the drying chamber walls and thereby enhancing recovery yield. Additionally, maltodextrin helps decrease the moisture content of the powder, contributing to the protection of chlorophyll against thermal degradation. However, excessively high maltodextrin levels may cause a slight decrease in recovery yield due to increased feed viscosity, which hinders atomization and evaporation processes. Moreover, the high solid content can lead to particle agglomeration inside the drying chamber, reducing powder collection efficiency in the cyclone system. Therefore, selecting an optimal maltodextrin concentration is critical to balance chlorophyll protection and process recovery efficiency [26]. In contrast, excessive maltodextrin resulted in higher solid content and viscosity of the feed, which hindered moisture evaporation and increased the residual moisture content in the final powder. In addition to yield, the appearance of the spray-dried powders also changed with varying maltodextrin concentrations. Higher maltodextrin levels produced powders that were finer, softer, non-sticky, and lighter in colour. These improvements are attributed to the inherent properties of maltodextrin, including its white colour, high molecular weight, and bulking characteristics [27]. The findings are consistent with previous studies that reported the significant influence of maltodextrin on both moisture content and recovery efficiency during spray drying processes [28]. The feed flow rate significantly influenced the recovery efficiency of chlorophyll powder during the spray drying process. Experimental results demonstrated that increasing the flow rate from 6 to 8 mL/min enhanced the recovery efficiency from $57.17 \pm 0.75\%$ to $64.12 \pm 1.17\%$. This relationship is clearly illustrated in Fig. 4B, which shows a positive correlation between feed flow rate and recovery efficiency within the investigated range. However, when the flow rate increased to 9 mL/min, the recovery efficiency decreased to $59.75 \pm 0.97\%$. A flow rate of 8 mL/min provided optimal recovery efficiency, likely due to a balance between the residence time of the material in the drying chamber and the evaporation rate of moisture. This is consistent with the findings of Seda Esus *et al.*, (2007), who reported a maximum recovery efficiency of 63% for spray-dried anthocyanin at a feed rate of 6.73 mL/min under the same drying temperature (160 °C) [29], highlighting that different compounds require specific feed rates to achieve comparable recovery outcomes. Increasing the inlet air temperature significantly influenced the moisture content and recovery efficiency of chlorophyll powder. As shown in Fig. 4C, recovery efficiency increased from $65.86 \pm 1.66\%$ at 140 °C to a maximum of $72.98 \pm 0.30\%$ at 160 °C, then declined to $69.29 \pm 1.41\%$ at 170 °C. At lower temperatures (≤ 150 °C), insufficient moisture evaporation due to a low-temperature gradient resulted in prolonged residence time and particle adhesion to chamber walls, reducing yield. The inlet temperature in the spray drying process plays a crucial role in balancing product recovery and powder quality, especially for heat-sensitive compounds such as chlorophyll. At 160 °C, both heat and mass transfer are optimized, facilitating rapid moisture evaporation and promoting the formation of a protective film around chlorophyll molecules. This film minimizes direct exposure of chlorophyll to heat and oxygen, thereby reducing degradation caused by thermal and oxidative processes and contributing to higher pigment retention. When the inlet temperature exceeds 160 °C, particle surfaces may reach or surpass their glass transition temperature (T_g), leading to stickiness and partial melting of powders on the drying chamber wall. This results in substantial powder loss and a decline in overall recovery yield. Moreover, excessive temperatures accelerate the breakdown of chlorophyll, further compromising its concentration in the final product. On the other hand, drying at temperatures below 160 °C leads to insufficient moisture removal, resulting in powder agglomeration and wall deposition due to higher water content, which adversely affects powder recovery and stability. Therefore, 160 °C is considered the optimal drying temperature, as it offers a favorable balance between effective moisture reduction, minimal chlorophyll degradation, and enhanced powder recovery, supported by both thermodynamic and physicochemical principles governing the spray drying process.

[30, 31, 32]. Conversely, excessive temperatures (≥ 170 °C) accelerate moisture loss but increase thermal degradation and product sticking, also reducing recovery. These findings align with those of Le Huong Thuy, who reported optimal powder quality at 164 °C for spray-dried chlorophyll [33]. Therefore, 160 °C was selected as the optimal inlet temperature, balancing recovery efficiency and product quality.

In short, the optimal spray drying parameters for chlorophyll powder production were identified as 25% carrier concentration, a feed rate of 8 mL/min, and an inlet temperature of 160 °C. Under these conditions, the highest recovery efficiency was achieved, reaching $72.98 \pm 0.30\%$. The spray-dried chlorophyll powder obtained under these optimal conditions will be further characterized using SEM, FT-IR, and XRD analyses to gain deeper insights into its morphology, functional groups, and crystalline structure.

3.4. Characterization of chlorophyll powder

The obtained chlorophyll powder was determined by physicochemical properties such as moisture, bulk density, particle density, porosity, flowability, solubility, and encapsulation efficiency. The results are shown in Table 4.

The moisture content of the spray-dried chlorophyll powder was $3.37 \pm 0.013\%$, which is below the commonly recommended threshold of 4–6% for food powders to ensure prolonged shelf life and reduced microbial activity. This result demonstrates the effectiveness of the optimized drying conditions and the role of maltodextrin in producing a low-moisture powder matrix, thereby enhancing product stability during storage. The bulk density (0.26 ± 0.002 g/cm³) and tapped density (0.37 ± 0.01 g/cm³) were relatively low, which is typical for powders produced using maltodextrin as the sole carrier. Additionally, the measured particle density was 0.87 ± 0.07 g/cm³, and the calculated porosity reached $58.02 \pm 1.84\%$, indicating a highly porous internal structure. This may be attributed to air entrapment during atomization and the weak film-forming ability of maltodextrin, which favours the formation of hollow or irregularly shaped particles [34]. As reported by Efraim *et al.*, (2013), amorphous solids increase the contact surface area between particles, thereby enhancing interparticle friction and compromising flowability [35]. Furthermore, surface roughness caused by irregular particle morphology can also increase frictional resistance and reduce flow behaviour [36]. The flowability of the powder was classified as poor, based on a CI of $28.95 \pm 2.80\%$ and a Hr of 1.41 ± 0.05 . These values are characteristic of powders with low interparticle cohesion and non-uniform morphology. Poor flow behaviour is often observed in carbohydrate-rich powders, such as those with high maltodextrin content, which tend to form low-density, amorphous particles with high surface roughness and frictional resistance [37]. Although maltodextrin plays a beneficial role in encapsulation and enhancing solubility, its impact on mechanical flow properties remains limited and should be considered in the formulation of food powders. Conversely, the powder exhibited high solubility ($87.09 \pm 1.93\%$), indicating excellent reconstitution behaviour in aqueous systems. This is a desirable attribute for applications in functional foods, particularly beverages and nutraceuticals. The high solubility is likely due to the hydrophilic nature of maltodextrin and the porous microstructure, which facilitates rapid water penetration and dispersion. These findings are in agreement with those of Ferrari *et al.*, (2012), who reported improved solubility in spray-dried fruit powders when maltodextrin was used as a carrier agent [38].

Table 4. Physicochemical properties of spray-dried chlorophyll powder

No.	Criteria	Unit	Results
1	Moisture	%	3.37 ± 0.01
2	Bulk density	g/cm ³	0.26 ± 0.002
3	Particle density	g/cm ³	0.87 ± 0.07
4	Tapped density	g/cm ³	0.37 ± 0.01
5	Flowability	CI (%)	28.95 ± 2.80
		HR	1.41 ± 0.05
6	Porosity	%	58.02 ± 1.84
7	Solubility	%	87.09 ± 1.93

3.4.1. Scanning electron microscopy (SEM)

The SEM of chlorophyll powder with two scale bars of 2 μm and 10 μm is shown in Fig. 5. The morphology of the powder particles reveals the presence of spherical particles with relatively smooth surfaces, characteristic of products formed from the spray drying process with the presence of maltodextrin as a carrier. Additionally, some irregular particles with sharp edges were observed, which may represent chlorophyll crystals that have not been fully encapsulated. This suggests that the spray drying process has produced a stable spherical structure that helps protect the active ingredient, although a small proportion of the substance has not been effectively encapsulated. The variation in droplet size during the spray drying process leads to differences in evaporation rate and the timing of membrane (skin) formation. Smaller droplets have a higher surface area-to-volume ratio and evaporate more quickly, causing the skin to form earlier. This limits shrinkage and results in spherical particles with smooth surfaces [39]. Moreover, the presence of particularly at low concentrations contributes to the formation of particles with a smooth appearance. This can be attributed to the characteristics of maltodextrin, a low molecular weight polysaccharide that acts as a plasticizer, reducing the uneven shrinkage of particle surfaces during the drying process [40].

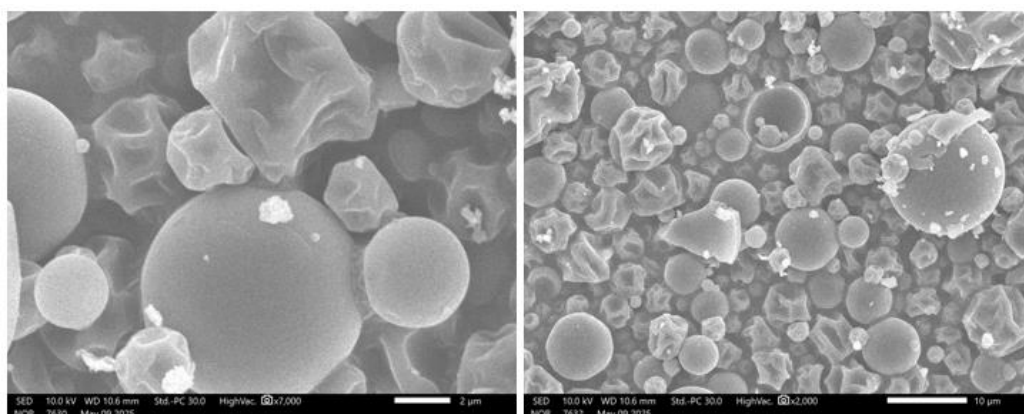


Figure 5. Micrographs of particles of the chlorophyll powder (SEM at $\times 7000$ (left) and at $\times 2000$ (right))

3.4.2. X-ray diffraction analysis (XRD)

The XRD pattern of the chlorophyll powder maltodextrin shows a broad, diffuse peak centred around $2\theta \approx 20^\circ$ (Fig. 6). This pattern is characteristic of amorphous materials, which exhibit a disordered molecular arrangement and, therefore, show low crystallinity [41]. There is an absence of sharp and well-defined diffraction peaks, especially those typically associated with crystalline chlorophyll, indicating that chlorophyll was effectively encapsulated within the maltodextrin matrix during spray drying. This structural transformation from a semi-crystalline to an amorphous form suggests successful entrapment of chlorophyll within the wall material, reducing its individual crystalline characteristics. These results are in agreement with previous studies, which reported that both gum arabic and maltodextrin - widely used wall materials - tend to form amorphous matrices after spray drying [42, 43]. This finding is consistent with the results of other studies [17, 44]. Furthermore, the amorphous nature of the spray-dried powder may positively influence its solubility and initial reconstitution properties. However, it should be noted that amorphous structures are generally more hygroscopic, which can lead to moisture absorption, microstructure collapse, or degradation of encapsulated compounds during storage [41, 45]. Despite this, encapsulation in maltodextrin may enhance the overall physical protection of chlorophyll and delay degradation. In conclusion, the XRD results confirm that the chlorophyll pigment underwent structural transformation during spray drying and is now primarily present in an amorphous state, likely embedded within the maltodextrin matrix. This structural configuration is expected to improve the handling and dispersion properties of the powder, although proper packaging is required to mitigate hygroscopic effects during storage.

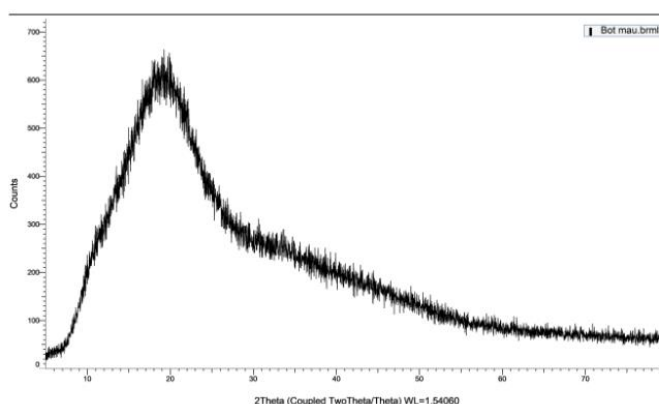


Figure 6. X-ray diffraction of the chlorophyll powder

3.4.3. FT-IR analysis

The FTIR spectrum of chlorophyll powder is presented in Figure 7. A broad band centred at approximately $3,300\text{ cm}^{-1}$ is attributed to O–H and N–H stretching vibrations [46], which are characteristic of hydroxyl groups in chlorophyll and the porphyrin ring structure. This band also indicates possible hydrogen bonding, potentially influenced by the presence of maltodextrin. A strong peak at $1,732\text{--}1,650\text{ cm}^{-1}$, which typically corresponds to C=O stretching in ester and keto groups of chlorophyll a, was not distinctly observed but may have overlapped with broader signals or reduced due to interactions with the carrier material [46]. However, a moderate band at $1,351\text{ cm}^{-1}$ is consistent with O–H bending vibrations, supporting the retention of hydroxyl functionalities [47]. The absorptions at $1,148\text{ cm}^{-1}$ and $1,021\text{ cm}^{-1}$ are associated with C–O–C and C–N stretching vibrations, suggesting the preservation of ether and amine functionalities in the chlorophyll structure, including those linked to the pyrrole rings of the porphyrin macrocycle [48]. A notable band at 575 cm^{-1} is attributed to Mg–N vibrations, confirming the integrity of the central magnesium ion complex within the chlorophyll molecule after processing [49]. Overall, the presence of key functional groups such as O–H, C–N, C–O, and Mg–N indicates that the chlorophyll structure remained largely intact after microwave-assisted extraction and spray-drying. The spectral data further support the successful incorporation and stabilization of chlorophyll in the maltodextrin matrix.

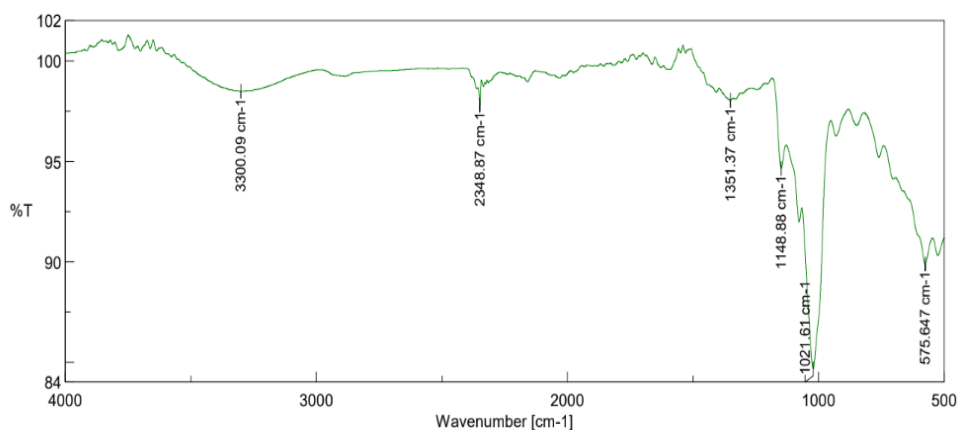


Figure 7. FT-IR spectra of the chlorophyll powder

3.4.4. Quality assessment of the chlorophyll powder

The results of heavy metal analysis showed that the concentrations of cadmium (0.04324 mg/kg), arsenic (0.948 mg/kg), lead (0.433 mg/kg), and mercury (0.030 mg/kg) were all within the maximum allowable limits established by Commission Regulation (EU No 23/2012) (Table 5).

The compliance with these limits indicates that the raw materials and the spray-drying process, including maltodextrin encapsulation, did not significantly contribute to heavy metal contamination in the final product. This is a crucial finding as heavy metals, particularly arsenic and lead, are toxic and can accumulate in the human body, potentially causing adverse health effects. Arsenic and lead are among the most strictly regulated metals due to their high toxicity and bioaccumulation potential in the food chain. The analyses were carried out in accordance with the AOAC 2015.01 standard method, ensuring the reliability and accuracy of the data. These results align with previous studies, which reported that the spray-drying process when combined with wall materials like maltodextrin. Typically, it does not result in significant heavy metal accumulation in the final dried product [50]. In terms of microbiological quality, the total aerobic microbial count was measured at 6.9×10^3 CFU/g, while the yeast and mould count were 7.6×10^3 CFU/g (Table 5). Although no specific microbiological limits from EU regulations were referenced in this study, these values are within typical ranges reported for spray-dried plant-based powders. However, the relatively high yeast and mould count suggests the need for improved hygiene control during post-drying handling and packaging to prevent potential degradation during storage. Fungal contamination not only impacts sensory quality and shelf-life but also poses a risk of mycotoxin production under certain conditions.

Table 5. Microbiological and heavy metal analysis results of chlorophyll powder.

No	Parameters	Unit	Results	Acceptable limit *	Methods
1	Total aerobic microbial count	CFU/g	6.9×10^3		ISO 4833-1:2013
2	Total yeast and mold count	CFU/g	7.6×10^3		ISO 21527-2:2008
3	Cadmium	mg/kg	0.04324	≤ 1 mg/kg	AOAC 2015.01
4	Arsenic	mg/kg	0.94750	≤ 3 mg/kg	
5	Lead	mg/kg	0.43307	≤ 5 mg/kg	
6	Mercury	mg/kg	0.03037	≤ 1 mg/kg	

*Commission Regulation (EU 23/2012)

Overall, the results of this study demonstrate that the spray-dried chlorophyll powder with maltodextrin encapsulation complies with the heavy metal safety limits outlined in EU regulations, reinforcing its potential as a functional food ingredient or additive. However, further attention is needed to control microbial contamination during the post-processing stages and packaging to ensure long-term stability and safety.

4. CONCLUSION

This study successfully optimized the extraction and spray drying processes to produce a stable, high-quality chlorophyll powder from the abundant and underutilized algae *C. aerea*. The optimal extraction conditions (0.8% MgCO_3 , 360 W, 240 s) combined with spray drying parameters (25% maltodextrin, 8 mL/min feed rate, 160 °C) achieved a high chlorophyll content and recovery efficiency of $79.98 \pm 3.753\%$. The product met microbiological and heavy metal safety standards, while structural analyses (SEM, FTIR, XRD) confirmed its quality and stability. This chlorophyll powder shows strong potential for applications in the functional food, natural colorant, and pharmaceutical markets. Importantly, utilizing *C. aerea* not only valorizes a locally abundant biomass resource but also contributes to environmental protection by mitigating the pollution caused by excessive seaweed growth. Future research will focus on evaluating the biological activities of the chlorophyll powder to further substantiate its health benefits and expand its commercial applications.

REFERENCES

1. Indrasti D., Andarwulan N., Purnomo E. H., and Wulandari N. U. R. - Stability of chlorophyll as natural colorant: a review for suji (*Dracaena angustifolia* (Medik.) Roxb.) leaves' case. Current

- Research in Nutrition and Food Science Journal **6** (3) (2018) 609-625.
<https://doi.org/10.12944/crnfsj.6.3.04>
2. Pareek S., Sagar N. A., Sharma S., Kumar V., Agarwal T., González-Aguilar G. A., and Yahia E. M. - Chlorophylls: Chemistry and biological functions. Fruit and Vegetable Phytochemicals: Chemistry and Human Health, 2nd Edition (2017) 269-284.
3. Humphrey A. M. - Chlorophyll. Food Chemistry **5** (1) (1980) 57-67.
[https://doi.org/10.1016/0308-8146\(80\)90064-3](https://doi.org/10.1016/0308-8146(80)90064-3)
4. Jorge A. M. S., Pedroso P. R. M., and Pereira J. F. B. - Sustainable extraction and utilization of chlorophyll from microalgae for eco-friendly wool dyeing. Journal of Cleaner Production **451** (2024). <https://doi.org/10.1016/j.jclepro.2024.142009>
5. Vijayaram S., Ringø E., Ghafarifarsani H., Hoseinifar S. H., Ahani S., and Chou C.-C. - Use of algae in aquaculture: a review. Fishes **9** (2) (2024). <https://doi.org/10.3390/fishes9020063>
6. Huang B., Teng L., and Ding L. - Morphological and molecular discrimination of green macroalgae *Chaetomorpha aerea* and *C. linum*. Acta Oceanologica Sinica **35** (4) (2016) 118-123. <https://doi.org/10.1007/s13131-016-0841-x>
7. Stephan H., Juran S., Antonioli B., Gloe K., and Gloe K. - Extraction methods. Analytical Methods in Supramolecular Chemistry (2006) 79-103.
8. Eskilsson C. S. and Bjorklund E. - Analytical-scale microwave-assisted extraction. Journal of Chromatography A **902** (1) (2000) 227-50. [https://doi.org/10.1016/S0021-9673\(00\)00921-3](https://doi.org/10.1016/S0021-9673(00)00921-3)
9. Pang X., Xu C., Jiang Y., Xiao Q., and Leung A. W. - Natural products in the discovery of novel sonosensitizers. Pharmacology & Therapeutics **162** (2016) 144-51.
<https://doi.org/10.1016/j.pharmthera.2015.12.004>
10. Abbas F., Zhou Y., O'Neill Rothenberg D., Alam I., Ke Y., and Wang H. C. - Aroma components in horticultural crops: chemical diversity and usage of metabolic engineering for industrial applications. Plants (Basel) **12** (9) (2023). <https://doi.org/10.3390/plants12091748>
11. Orthesin N., Hidayat I. T., Wahyuni W. T., Syafitri U. D., Herbani Y., and Sari Y. W. - Optimization of chlorophyll extraction from dried *Spirulina platensis* using low power microwave assisted extraction method. IOP Conference Series: Earth and Environmental Science **1359** (1) (2024). <https://doi.org/10.1088/1755-1315/1359/1/012021>
12. Georgiopoulou I., Tzima S., Louli V., and Magoulas K. - Process optimization of microwave-assisted extraction of chlorophyll, carotenoid and phenolic compounds from *Chlorella vulgaris* and comparison with conventional and supercritical fluid extraction. Applied Sciences **13** (4) (2023). <https://doi.org/10.3390/app13042740>
13. Graff J. R. and Rynearson T. A. - Extraction method influences the recovery of phytoplankton pigments from natural assemblages. Limnology and Oceanography: Methods **9** (4) (2011) 129-139. <https://doi.org/10.4319/lom.2011.9.129>
14. Amilia W., Wiyono A. E., Shasabilah R. T., Choiron M., and Belgis M. - Physical and chemical characteristics of cassava leaf chlorophyll as natural dye powder (*Manihot esculenta* Crantz) with tween 80 and alkaline type variations. International Journal on Food, Agriculture and Natural Resources **4** (1) (2023) 27-33. <https://doi.org/10.46676/ij-fanres.v4i1.137>
15. Ledari S. A., Milani J. M., Shahidi S. A., and Golkar A. - Fabrication and optimization of ultra-long stable microencapsulated chlorophyll using combinations of wall material via response surface methodology. Heliyon **10** (22) (2024) e40161.
<https://doi.org/10.1016/j.heliyon.2024.e40161>
16. Mohd Amin S. F., Muhammad K., Yusof Y. A., Abdul Aziz A. H., and Mohd Noor N. Q. I. - Kinetic degradation and colour stability in an aqueous system of spray-dried metal-stabilised amaranth powder encapsulated in different wall materials. Malaysian Journal of Fundamental and Applied Sciences **21** (1) (2025) 1726-1739. <https://doi.org/10.11113/mjfas.v21n1.3664>
17. Zhang Z.-H., Peng H., Woo M. W., Zeng X.-A., Brennan M., and Brennan C. S. - Preparation and characterization of whey protein isolate-chlorophyll microcapsules by spray drying: Effect of WPI

- ratios on the physicochemical and antioxidant properties. *Journal of Food Engineering* **267** (2020). <https://doi.org/10.1016/j.jfoodeng.2019.109729>
18. Idham Z., Muhamad I. I., and Sarmidi M. R. - Degradation kinetics and color stability of spray-dried encapsulated anthocyanins from *Hibiscus Sabdariffa* L. *Journal of Food Process Engineering* **35** (4) (2011) 522-542. <https://doi.org/https://10.1111/j.1745-4530.2010.00605.x>
 19. Fang Z. and Bhandari B. - Comparing the efficiency of protein and maltodextrin on spray drying of bayberry juice. *Food Research International* **48** (2) (2012) 478-483. <https://doi.org/10.1016/j.foodres.2012.05.025>
 20. Saifullah M., Yusof Y. A., Chin N. L., and Aziz M. G. - Physicochemical and flow properties of fruit powder and their effect on the dissolution of fast dissolving fruit powder tablets. *Powder Technology* **301** (2016) 396-404. <https://doi.org/10.1016/j.powtec.2016.06.035>
 21. Santhalakshmy S., Don Bosco S. J., Francis S., and Sabeena M. - Effect of inlet temperature on physicochemical properties of spray-dried jamun fruit juice powder. *Powder Technology* **274** (2015) 37-43. <https://doi.org/10.1016/j.powtec.2015.01.016>
 22. Porra R. J. - The chequered history of the development and use of simultaneous equations for the accurate determination of chlorophylls a and b. *Photosynthesis Research* **73** (1-3) (2002) 149-156.
 23. Anandharamakrishnan C., Rielly C. D., and Stapley A. G. F. - Loss of solubility of α -lactalbumin and β -lactoglobulin during the spray drying of whey proteins. *LWT - Food Science and Technology* **41** (2) (2008) 270-277. <https://doi.org/10.1016/j.lwt.2007.03.004>
 24. Nguyen N. H. K., An N. T. D., Anh P. K., and Truc T. T. - Microwave-assisted extraction of chlorophyll and polyphenol with antioxidant activity from *Pandanus amaryllifolius* Roxb. in Vietnam. *IOP Conference Series: Materials Science and Engineering* **1166** (1) (2021). <https://doi.org/10.1088/1757-899x/1166/1/012039>
 25. Tong Y., Gao L., Xiao G., and Pan X. - Microwave pretreatment-assisted ethanol extraction of chlorophylls from *Spirulina platensis*. *Journal of Food Process Engineering* **35** (5) (2011) 792-799. <https://doi.org/10.1111/j.1745-4530.2010.00629.x>
 26. Fazaeli M., Emam-Djomeh Z., Kalbasi Ashtari A., and Omid M. - Effect of spray drying conditions and feed composition on the physical properties of black mulberry juice powder. *Food and Bioproducts Processing* **90** (4) (2012) 667-675. <https://doi.org/10.1016/j.fbp.2012.04.006>
 27. Bae E. K. and Lee S. J. - Microencapsulation of avocado oil by spray drying using whey protein and maltodextrin. *Journal of Microencapsulation* **25** (8) (2008) 549-60. <https://doi.org/10.1080/02652040802075682>
 28. Azhar M. D., Ibrahim U. K., Zaki N. A. M., and Hashib S. A. - The effect of maltodextrin concentration and inlet air temperature on spray dried *Centella Asiatica* L. powder. *IOP Conference Series: Materials Science and Engineering* **736** (3) (2020). <https://doi.org/10.1088/1757-899x/736/3/032017>
 29. Ersus S. and Yurdagel U. - Microencapsulation of anthocyanin pigments of black carrot (*Daucus carota* L.) by spray drier. *Journal of Food Engineering* **80** (3) (2007) 805-812. <https://doi.org/10.1016/j.jfoodeng.2006.07.009>
 30. Nayaka V. S. K., Azeez S., Suresha G. J., Tiwari R. B., Prasanth S. J., Karunakaran G. S., and Suresha K. B. - Influence of intel drying temperature on the physical attributes of spray dried avocado (*Persea americana* Mill) powder. *International Journal of Current Microbiology and Applied Sciences* **9** (12) (2020) 1761-1770. <https://doi.org/10.20546/ijemas.2020.912.208>
 31. Tuyen K. C. and Trang H. P. P. - Spray-drying microencapsulation of polyphenols by polysaccharide from yeast cell walls. *Ho Chi Minh City Open University Journal Of Science-Engineering And Technology* **12** (1) (2022) 79-89. <https://doi.org/10.46223/HCMCOUJS.tech.en.12.1.2028.2022>
 32. Dat L. Q. - Influences of maltodextrin and hot air temperature on losses of betacyanin and antioxidant capacity in beetroot juice spray drying. *Vietnam Journal of Science and Technology* **55** (5A) (2018). <https://doi.org/10.15625/2525-2518/55/5a/12183>

33. Thuy L. H. - Study on processing for instant *Caulerpa lentilliera* algae powder. *Journal of Science and Technology-IUH* **44** (02) (2020).
34. Tonon R. V., Brabet C., and Hubinger M. D. - Anthocyanin stability and antioxidant activity of spray-dried açai (*Euterpe oleracea* Mart.) juice produced with different carrier agents. *Food Research International* **43** (3) (2010) 907-914. <https://doi.org/10.1016/j.foodres.2009.12.013>
35. Efraim P., Barreto Alves A., and Calil Pereira Jardim D. - Revisão: Polifenóis em cacau e derivados: teores, fatores de variação e efeitos na saúde. *Brazilian Journal of Food Technology* **14** (03) (2011) 181-201. <https://doi.org/10.4260/bjft2011140300023>
36. Lopes Neto J. P., Nascimento J. W. B. d., and Fank M. Z. - Forças verticais e de atrito em silos cilíndricos com fundo plano. *Revista Brasileira de Engenharia Agrícola e Ambiental* **18** (6) (2014) 652-657. <https://doi.org/10.1590/s1415-43662014000600013>
37. Hoang N. T. N., Nguyen N. N. K., Nguyen L. T. K., Le A. T. H., and Dong D. T. A. - Research on optimization of spray drying conditions, characteristics of anthocyanins extracted from *Hibiscus sabdariffa* L. flower, and application to marshmallows. *Food Science & Nutrition* **12** (3) (2024) 2003-2015. <https://doi.org/10.1002/fsn3.3898>
38. Ferrari C. C., Germer S. P. M., Alvim I. D., Vissotto F. Z., and de Aguirre J. M. - Influence of carrier agents on the physicochemical properties of blackberry powder produced by spray drying. *International Journal of Food Science & Technology* **47** (6) (2012) 1237-1245. <https://doi.org/10.1111/j.1365-2621.2012.02964.x>
39. van Boven A. P., Siemons I., Kohlus R., and Schutyser M. A. I. - Analysis on particle morphology development during pilot-scale spray drying of maltodextrins. *Drying Technology* **43** (5) (2025) 840-857. <https://doi.org/10.1080/07373937.2025.2472390>
40. da Silva Carvalho A. G., da Costa Machado M. T., da Silva V. M., Sartoratto A., Rodrigues R. A. F., and Hubinger M. D. - Physical properties and morphology of spray dried microparticles containing anthocyanins of jussara (*Euterpe edulis* Martius) extract. *Powder Technology* **294** (2016) 421-428. <https://doi.org/10.1016/j.powtec.2016.03.007>
41. Nambiar R. B., Sellamuthu P. S., and Perumal A. B. - Microencapsulation of tender coconut water by spray drying: effect of *Moringa oleifera* gum, maltodextrin concentrations, and inlet temperature on powder qualities. *Food and Bioprocess Technology* **10** (9) (2017) 1668-1684. <https://doi.org/10.1007/s11947-017-1934-z>
42. Silva K. A., Coelho M. A. Z., Calado V. M. A., and Rocha-Leão M. H. M. - Olive oil and lemon salad dressing microencapsulated by freeze-drying. *LWT - Food Science and Technology* **50** (2) (2013) 569-574. <https://doi.org/10.1016/j.lwt.2012.08.005>
43. Botrel D. A., de Barros Fernandes R. V., Borges S. V., and Yoshida M. I. - Influence of wall matrix systems on the properties of spray-dried microparticles containing fish oil. *Food Research International* **62** (2014) 344-352. <https://doi.org/10.1016/j.foodres.2014.02.003>
44. Martínez J. R., Vázquez-Durán A., Martínez-Castañón G., Ortega-Zarzosa G., Palomares-Sánchez S. A., and Ruiz F. - Coesite formation at ambient pressure and low temperatures. *Advances in Materials Science and Engineering* **2008** (2008) 1-6. <https://doi.org/10.1155/2008/406067>
45. Borrmann D., Pierucci A. P., Leite S., and Leão M. H. - Microencapsulation of passion fruit (*Passiflora*) juice with n-octenylsuccinate-derivatised starch using spray-drying. *Food and Bioprocess Processing* **91** (1) (2013) 23-27. <https://doi.org/10.1016/j.fbp.2012.08.001>
46. Breton J., Navedryk E., and Leibl W. - FTIR study of the primary electron donor of photosystem I (P700) revealing delocalization of the charge in P700(+) and localization of the triplet character in (3)P700. *Biochemistry* **38** (36) (1999) 11585-92. <https://doi.org/10.1021/bi991216k>
47. Kang Y. R., Lee Y. K., Kim Y. J., and Chang Y. H. - Characterization and storage stability of chlorophylls microencapsulated in different combination of gum Arabic and maltodextrin. *Food Chem* **272** (2019) 337-346. <https://doi.org/10.1016/j.foodchem.2018.08.063>
48. Kurniasih R. A., Dewi E. N., and Purnamayati L. - Effect of different coating materials on the characteristics of chlorophyll microcapsules from *Caulerpa racemosa*. *IOP Conference Series: Earth and Environmental Science* **116** (2018). <https://doi.org/10.1088/1755-1315/116/1/012030>

49. Coquillat D., O'Connor E., Brouillet E. V., Meriguet Y., Bray C., Nelson D. J., Faulds K., Torres J., and Dyakonova N. - Terahertz vibrational modes of sodium magnesium chlorophyllin and chlorophyll in plant leaves. *Journal of Infrared, Millimeter, and Terahertz Waves* **44** (3-4) (2023) 245-264. <https://doi.org/10.1007/s10762-023-00905-6>
50. Homayouni Rad A., Pirouzian H. R., Toker O. S., and Konar N. - Application of simplex lattice mixture design for optimization of sucrose-free milk chocolate produced in a ball mill. *LWT* **115** (2019). <https://doi.org/10.1016/j.lwt.2019.108435>

TÓM TẮT

NGHIÊN CỨU TRÍCH LY VÀ SẤY PHUN THU NHẬN BỘT GIÀU CHLOROPHYLL TỪ RONG *Chaetomorpha aerea*

Hoàng Thị Ngọc Nhon*, Nguyễn Hoàng Bảo Ngân, Hồ Phùng Thanh Doanh

Trường Đại học Công Thương Thành phố Hồ Chí Minh

*Email: nhonhtn@huut.edu.vn

Chaetomorpha aerea là một loài tảo lục dạng sợi, thường phân bố ở các môi trường nuôi trồng thủy sản có độ mặn hoặc lợ. Sự phát triển quá mức của loài này có thể gây ra những vấn đề sinh thái và ảnh hưởng đến hoạt động vận hành. Việc tận dụng sinh khối phong phú này để chiết xuất chlorophyll không chỉ góp phần giảm thiểu tác động môi trường mà còn mở ra hướng tiếp cận bền vững nhằm thu hồi các hợp chất sinh học có giá trị cao, do loài này có hàm lượng chlorophyll tương đối lớn. Chlorophyll là một sắc tố tự nhiên thiết yếu trong quá trình quang hợp, hiện được ứng dụng rộng rãi như một chất phụ gia chức năng trong ngành thực phẩm và mỹ phẩm nhờ các đặc tính chống oxy hóa, kháng khuẩn, kháng nấm, chống ung thư. Nghiên cứu này khảo sát ảnh hưởng của nồng độ $MgCO_3$, công suất vi sóng và thời gian chiết đến hiệu suất chiết xuất chlorophyll từ *C. aerea* bằng phương pháp chiết xuất hỗ trợ vi sóng (MAE). Thiết kế Box-Behnken được áp dụng để tối ưu hóa các điều kiện chiết, kết quả tối ưu thu được là 0,8% $MgCO_3$, 360 W và 240 giây, cho hàm lượng chlorophyll đạt 50,831 $\mu g/mL$, phù hợp với giá trị dự đoán từ mô hình. Dịch chiết sau đó được cô đặc chân không ở 48 °C đến khi đạt hàm lượng chất khô 12%, sau đó phối trộn với maltodextrin ở tỷ lệ 25% và sấy phun ở 160 °C với tốc độ cấp liệu 8 mL/phút. Sản phẩm bột cuối cùng thu được có màu xanh, độ ẩm 3,37%, khả năng hòa tan tốt trong nước và hiệu suất thu hồi đạt 72,98%. So với các nghiên cứu trước đó, phương pháp MAE giúp tăng hàm lượng chlorophyll khoảng 1,5 lần, trong khi sấy phun gần như tăng gấp đôi hiệu suất thu hồi, cho thấy hiệu quả của chiến lược tích hợp giữa chiết xuất và ổn định hóa sản phẩm.

Từ khóa: Box-behnken, *Chaetomorpha aerea*, chlorophyll, tối ưu, sấy phun.